# Improved Image Fusion Using Balanced Multiwavelets

Lahouari Ghouti, Ahmed Bouridane and Mohammad K. Ibrahim

*Abstract*— **This paper presents the use of balanced multiwavelets for image fusion. The proposed image fusion scheme incorporates the use of balanced multiwavelets transform, which uses multiple wavelet and scaling functions for the first time. Wavelet-based fusion techniques have been successfully applied to combine perceptually important image features because the sensitivities of the human visual system (HVS) can be efficiently incorporated in the design of wavelets. Balanced multiwavelets have attracted attention for their desirable properties since they can simultaneously achieve symmetry, orthogonality, compact support and approximation order higher than one. Hence, filters with shorter length are used yielding lower computational complexity than scalar wavelet.**

## I. Introduction

With the availability of multi-sensor data in many disparate fields such as remote sensing, machine vision, robotics, medical imaging, and military application, effective sensor/data fusion has received much attention in the literature. In multi-sensor image, each of the input images conveys important information that cannot be discarded.

Image fusion can take place at the signal, pixel, feature, transform, and symbol level. Fusion techniques range from the simplest method of pixel averaging to more sophisticated and state-of-the-art methods such as multiresolution- and neural networks-based fusion. Initially, multi-sensor images must be correctly aligned on a pixel-by-pixel basis [1] for an effective and successful fusion.

Usually, more generic requirements are imposed on the fusion outcome such that: All relevant information in the input images must be preserved in the resulting image to satisfy the ”information-preserving” rule [2]. Any irrelevant details such as noise should be discarded from the result. The human visual system (HVS) is primarily sensitive to moving light stimuli. Any artifacts or inconsistency that would distract the human observer should be also suppressed. The fusion scheme, being employed, should not introduce such artefacts.

In this paper, the fusion based on balanced multiwavelets is introduced for the first time. The results clearly demonstrate the advantages of this approach. The paper is organized as follows: In section 2, we briefly review a generic multiresolution fusion scheme and then we will introduce and motivate the use of balanced multiwavelets in image fusion. In section 3, we introduce the stages of the proposed fusion algorithm. Experimental results of the proposed method are shown in section 4. Then, the proposed fusion is scheme is compared to a similar one based on unbalanced multiwavalets. Finally, conclusions are outlined in Section 5.

L. Ghouti is with the Information and Computer Science Department. King Fahd University of Petroleum and Minerals, Dhahran 31261, Saudi Arabia and the School of Computer Science, Queen’s University of Belfast, BTN 1NN, UK. Email: ghouti@ccse.kfupm.edu.sa

A. Bouridane is with the School of Computer Science, Queen’s University of Belfast, BTN 1NN, UK. Email: A.Bouridane@qub.ac.uk

M. K. Ibrahim is with the Computer Engineering Department. King Fahd University of Petroleum and Minerals, Dhahran 31261, Saudi Arabia. Email: ibrahimm@ccse.kfupm.edu.sa

## II. Image Fusion: Scalar Wavelets and Unbalanced Multiwavelets

The basic idea of multiresolution-based fusion techniques is motivated by the ability of the wavelet transform to take into account the properties of the HVS functionality. Wavelet decomposition allows the extraction of important image features such as edges [3]. Edges and corners are examples of local contrast changes to which the HVS is primary sensitive. Based on this motivation, wavelet-based fusion performs the combination of the important image features such as edges in the source images. The fusion process will produce a fused image that retains all the most salient features of the source images.

### A. Scalar Wavelet Fusion

A straightforward approach to image fusion is to compute the average of the source images pixel-wise. Despite the simplicity of this approach, the low contrast of the fused image seriously limits its use. To circumvent this limitation, multiresolution-based approaches are proposed for image fusion. The basic idea of all wavelet-based fusions schemes is to combine all respective wavelet coefficients from the input images. The combination is performed according to a specific fusion rule [1]. The wavelet decomposition of each source image $f_i(m,n)$ is performed leading to a multiresolution representation. The actual fusion process is performed as a combination of the corresponding wavelet decomposition coefficients of all input images, to build a single wavelet decomposition image. This combination takes place on all decomposition levels $k$ ($k = 1, 2, \ldots, L$) where $L$ is the maximum wavelet decomposition level. Two different fusion rules are applied to combine the most important features of the input images. A basic fusion rule is applied to the Lth-level approximation subbands. The three detail subbands (horizontal, vertical, and diagonal) are combined using a more sophisticated fusion algorithm as explained in Section 3. The procedure for merging two source images using scalar wavelet decomposition is illustrated in Figure 1.

Typical multiresolution decompositions include pyramid transforms such as the Laplacian pyramid, gradient pyramid, ratio of lowpass pyramid, and discrete scalar wavelet transform [3]. Burt [4] first proposed a multiscale approach for binocular fusion in human stereo vision. The proposed implementation is based on Laplacian pyramid and "*maximum*" selection rule. Similar schemes, based on the wavelet transform and using different combination rules, have been proposed [5].

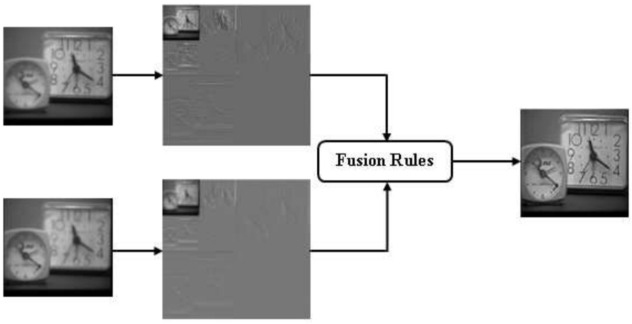


Figure 1: Image fusion process using scalar wavelet decomposition.

### *B. Unbalanced Multiwavelets Wavelet Fusion*

Multiwavelets are very similar to scalar wavelets but have some important differences. In contrast to scalar wavelets, which are described in the context of multiresolution analysis with a unique scaling function and a wavelet function, multiwavelets may have two or more scaling (and wavelet) functions. Goodman and Lee [6] are among the earliest to develop a multiresolution theory of multiwavelets. In his PhD work, Strela [7] further extends the theory of multiwavelets. He successfully presented it in terms of perfect reconstruction multifilter banks in both time and frequency domains. In the case of multiwavelets, the set of scaling functions can be written using the vector notation $\Phi(t) \equiv [\phi_1(t)\,\phi_2(t)\cdots\phi_r(t)]^T$ where $\Phi(t)$ is called the multiscaling function. Likewise, the multiwavelet function is defined from the set of wavelet functions as $\Psi(t) \equiv [\psi_1(t)\,\psi_2(t)\cdots\psi_r(t)]^T$. The scalar wavelet case is represented by $r = 1$. The values taken by the parameter $r$ can be arbitrarily large; we will restrict $r$ to 2 in this paper. The multiwavelet two-scale equations are similar to those of wavelets [7]:

$$\Phi(t) = \sqrt{2}\sum_{k=-\infty}^{\infty} H_k \Phi(2t-k) \tag{1}$$

$$\Psi(t) = \sqrt{2}\sum_{k=-\infty}^{\infty} G_k \Phi(2t-k) \tag{2}$$

It is worth noting that $\{H_k\}$ and $\{G_k\}$ are matrix filters, i.e., $H_k$ and $G_k$ are $r \times r$ matrices for each integer $k$. In contrast to the case of wavelets, the input and output of every branch in the multifilter bank is a vector. Figure 2 illustrates a single analysis/synthesis stage of multiwavelet processing. Each filter block in Figure 2 is really a 2-input/2-output system.

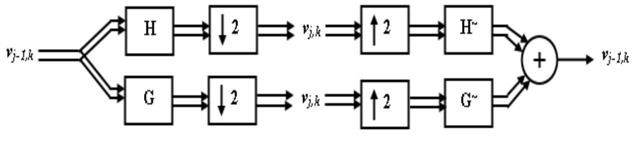


Figure 2: Analysis/synthesis stage of a single-level biorthogonal multiwavelet processing.

Many motivations lie behind the emergence of multiwavelets in signal and image processing applications. First, the extra degrees of freedom inherent in multiwavelets can be used to reduce restrictions on the filter properties. For example, it is well known that a scalar wavelet cannot simultaneously have both orthogonality and a symmetric impulse response that has length greater than 2. Symmetric filters are necessary for symmetric signal extension, while orthogonality makes the transform easier to design and implement. Following these motivations, Wang et al. [8] propose a scheme for pixel-level fusion using discrete multiwavelet transform. Multiwavelet decomposition is quite different from that based on scalar wavelets as shown in Figure 3.

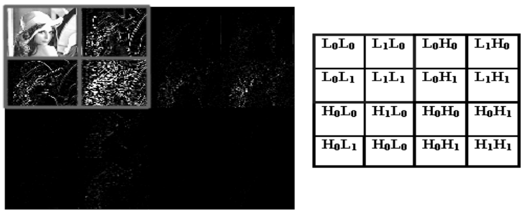


Figure 3: Single-level decomposition of Lena image using GHM mulitwavelet transform.

Figure 3 shows a single-level decomposition of Lena image using discrete Geronimo-Hardin-Massopust (GHM) multiwavelet transform. Unlike scalar wavelets, each decomposition level consists of 16 subbands. For instance, the lowpass subband consists of four blocks as illustrated in the right side of Figure 3. These local subbands, characterized by different spectral properties, make $L$-level decomposition using discrete multiwavelet look like $L+1$-level decomposition using discrete scalar wavelet [10].

In [8], the four blocks of the lowpass subbands are combined using the same fusion rule. It is clear that this approach does not take into account the spectral dissimilarity of these blocks. On the other hand, the detail subbands (horizontal, vertical, and diagonal) consist of blocks having similar spectral content. Hence, a shuffling procedure [11] can be applied on the blocks of the three detail subbands. Figure 4 confirms that shuffling cannot be applied to the blocks of the lowpass subband. In the next section, we propose the use of balanced multiwavelets [10] for improved image fusion. These latter yield subbands having blocks with similar spectral content. Thus, shuffling can applied equally.

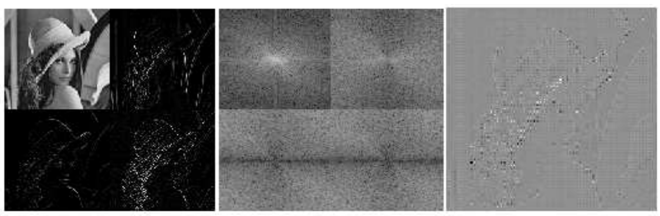

Figure 4: Lowpass subband of Lena image (left). Blocks' spectral content (center). Lowpass subband after shuffling (right).

## III. Image Fusion Using Balanced Multiwavelets

In general, for multiwavelets, the preservation property does not automatically follow from the vanishing moments property. But, for the balanced multiwavelet filter banks, both the preservation and annihilation properties hold. The balanced multiwavelets do not require a pre-processing stage (other than polyphase vectorization) for the input. If the lowpass/highpass branches of the filter bank preserve/annihilate polynomials of order less than $p$ where $p \leq K$, then the balancing order for the multiwavelet is $p$. A balancing order of $p$ implies at least $p$ vanishing moments; it also implies that ($0^{th}$, $1^{st}$, $2^{nd}$, $\ldots$, $(p-1)^{th}$) order polynomials are eigensignals of the lowpass branch band-Toeplitz matrix [10].

Figure 5 shows Figure 5 shows the lowpass and highpass branch outputs of a balanced multiwavelet filter bank (BAT-2 family [10]) for first order (ramp) input. It is clear that the input signal is preserved at the lowpass output while it is annihilated by the highpass branch. Symmetric signal extension contributes to the smoothness of the boundary points of the lowpass and highpass signals.

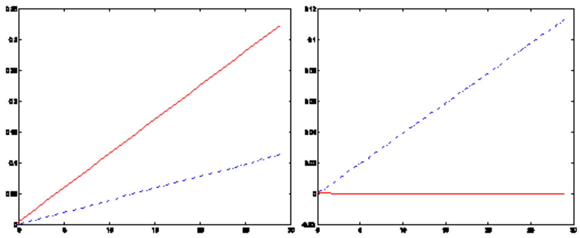

Figure 5: Decomposition using a second-order balanced multiwavelet of a ramp signal. Input signal (dotted blue) and branch output (solid red).

Selesnick [12], Lebrun and Vetterli [10] propose various constructions of balanced multiwavelet families. A balanced version of GHM multiwavelets is presented in [13]. During our work, we tested most of the proposed balanced multiwavelets. Most of them yielded similar performance for the image fusion problem. Balanced multiwavelets can be implemented using time-varying filter banks [10]. This implementation produces a signal representation identical to that obtained using scalar wavelets. Figure 6 shows the adopted implementation.

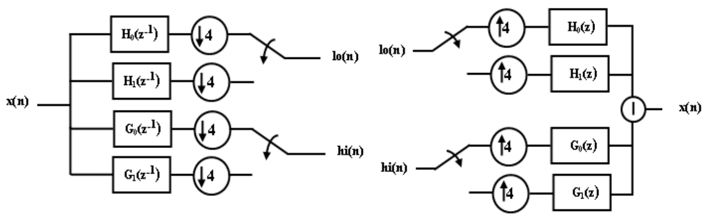


Figure 6: The time-varying balanced orthogonal multiwavelet filter bank. Analysis section (left). Synthesis section (right).

Like scalar wavelets, 2D balanced transform is separable. Hence, it can be defined as the tensor product of two 1D transforms. Figure 7 shows a single-level decomposition of Lena image using balanced multiwavelet transform (Bat-1 [10] multifilters). As expected, the blocks of the lowpass subband have similar spectral content.

As expected, shuffling can be safely applied to the blocks of the lowpass subband to yield a single-block lowpass subband similar to that obtained using scalar wavelets[1] (see Figure

[1] The shuffling process contributes to use exactly the same fusion procedure as that used with scalar wavelets.

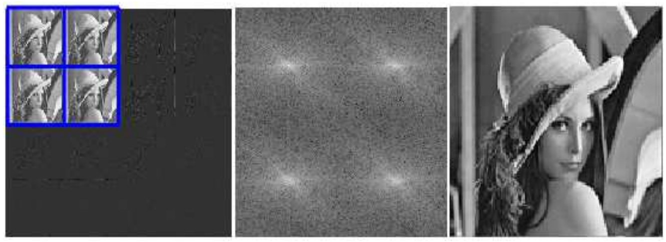

Figure 7: Single-level decomposition of Lena image using balanced BAT-1 mulitwavelet transform (left). Lowpass spectral content (center). Lowpass subband after shuffling (right).

7). Thus, balanced multiwavelets can now be compared to scalar wavelets on equal footing in practical image fusion applications.

Please note that we assume that the source images are "*perfectly*" registered since they are be obtained from different sensors having different resolutions. In the proposed fusion scheme, we apply the discrete balanced multiwavelet transform to each source image to create fused images that retain the most important features pertaining to all the source images. The captured features will then be exploited for human visual perception, object detection and target recognition. Except for the lowpass subband, all other subbands contain transform values that fluctuate around zero [8]. While the lowpass subband is an approximation of the input image, the three detail subbands convey information about the detail parts in horizontal, vertical and diagonal directions. Different merging procedures will be applied to approximation and detail subbands. Lowpass subbands will be merged using simple averaging operations since they both contain approximations of the source images. A selection procedure will be applied to the multiwavelet coefficients of the three detail subbands. The implemented selection allows for picking up the most salient features in these subbands for each source image. Figure 8 shows an image fusion scheme based on balanced multiwavelet decomposition as proposed in this paper. It is worth noting that Figure 8 shows a single-level balanced multiwavelet decompostion for illustration purposes. In practical situations, we usually use three-level decomposition.

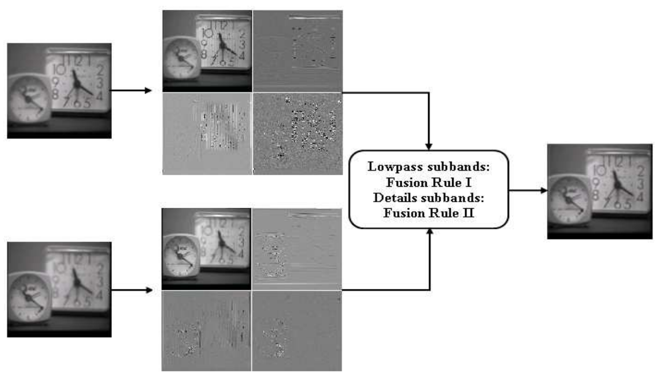


Figure 8: Proposed fusion scheme using balanced multiwavelets.

To provide a measure for image saliency, all transform coefficients in the detail subbands will be convolved with feature extracting operators $\mathbf{P_1}$, $\mathbf{P_2}$ and $\mathbf{P_3}$, respectively [8]. $\mathbf{P_1}$, $\mathbf{P_2}$ and $\mathbf{P_3}$ are designed to extract the edge information in the horizontal, vertical and diagonal detail subbands, respectively. They are defined as follows [8]:

$$\mathbf{P_1} = \begin{bmatrix} -1 & -1 & -1 \\ 2 & 2 & 2 \\ -1 & -1 & -1 \end{bmatrix} \quad \mathbf{P_2} = \begin{bmatrix} -1 & 2 & -1 \\ -1 & 2 & -1 \\ -1 & 2 & -1 \end{bmatrix}$$
$$\mathbf{P_3} = \begin{bmatrix} -1 & 0 & -1 \\ 0 & 4 & 0 \\ -1 & 0 & -1 \end{bmatrix} \tag{3}$$

## IV. Simulation and Experimental Results

Performance analysis of the proposed algorithm is summarized in this section. The set of test images consists of several pairs of natural images. The first two image pairs were taken using a Sony digital still camera MVC-FD7[2]. Figure 9 shows two pairs of test images with opposite side focus.

Figure 9: Test images with left focus (left column) and right focus (right column).

To compare fusion effects, several other methods were used to fuse the source images. The fused images using the proposed method are shown in Figure 10. Table I shows a summary of the performance of many fusion schemes to fuse the second pair of images shown in Figure 9 (second row). A subjective fusion quality measure can be provided by comparing the original image[3] with the fused image. For such comparisons, we will use the universal image quality index provided by Wang and Bovic [14]. An index value closer to 1 indicates better perceptual quality of the fused image. Figure 10 and Table I clearly demonstrate that the proposed fusion algorithm provides fused images with the best visual quality.

Figure 10: Fused images using proposed algorithm.

| Fusion Algorithm | Universal Quality Index |
|---|---|
| Simple Averaging | 0.7952 |
| Principal Component Analysis | 0.7962 |
| Maximum Selection | 0.7439 |
| Minimum Selection | 0.7497 |
| Laplacian Pyramid | 0.8259 |
| Gradient Pyramid | 0.7718 |
| DWT (Daubechies Basis) | 0.8178 |
| Shift-Invariant DWT (Haar Basis) | 0.8433 |
| Unbalanced multiwavelet (GHM [8]) | 0.7971 |
| Balanced multiwavelets (Bat-1 [10]) | **0.8651** |

Table I: Performance of several fusion algorithms: Fusion quality.

## V. Conclusion

In this paper, it is demonstrated how the performance of multiresolution-based image fusion can be increased significantly through the use of balanced multiwavelets. Balancing is essential to multiwavelet transform. Balanced multiwavelets have smoother basis functions allowing better quality for image fusion. The improved performance of the novel image fusion scheme is demonstrated using experimental images. The proposed scheme is compared to other fusion algorithms where results clearly indicate the superior performance of the former in terms of fused image quality using universal quality index.

**Acknowledgment:** L. Ghouti and M. K. Ibrahim acknowledge the support of KFUPM University.

## References


[1] H. Li, B. S. Manjunath and S. K. Mitra, "Multisensor image fusion using the wavelet transform," Graphical Models and Image Processing, Vol. 57, No. 3, pp. 235245, May 1995.

[2] S. Haykin, *Neural Networks: A Comprehensive Foundation*, Prentice Hall, Second Edition, 1999.

[3] S. Mallat, *A Wavelet Tour of Signal Processing*, Acaemic Press, Second Edition, 1998.

[4] P. J. Burt and R. J. Lolczynski, "Enhanced image capture through fusion," in Proc. of the 4th Intl. Conf. on Computer Vision, pp. 173182, Berlin, Germany, May 1993.

[5] A. Toet, "Hierarchical image fusion," Machine Vision App., pp. 1-11, March 1990.

[6] T. N. T. Goodman and S. L. Lee, "Wavelets of Multiplicity r," Trans. of the Amer. Math. Soc., Vol. 342, pp. 307-324, 1994.

[7] V. Strela, "Multiwavelets: Theory and Applications," Ph.D Thesis, MIT, 1996.

[8] H. Wang, J. Peng, and W. Wu, "Fusion algorithm for multisensor images based on discrete multiwavelet transform," IEE Proc. Vis. Image Signal Process., Vol. 149, No. 5, pp. 283-289, Oct. 2002.

[9] K. Kazemi and H. A. Moghaddam, "Fusion of multifocus images using discrete multiwavelet transform," IEEE Conf. on Multisensor Fusion and Int. for Int. Systems, pp. 167-172, 2003.

[10] J. Lebrun and M. Vetterli, "Balanced multiwavelets theory and design," IEEE Trans. on Signal Processing, Vol. 46, No. 4, pp. 1119-1124, Apr. 1998.

[11] M. B. Martin and A. E. Bell, "New image compression techniques using multiwavelets and multiwavelet packets," IEEE Trans. on Image Processing, Vol. 10, No. 4, pp. 500-511, Apr. 2001.

[12] I. Salesnick, "Multiwavelet bases with extra approximation properties," IEEE Trans. on Signal Processing, Vol. 46, No. 11, pp. 2898-2908, Nov. 1998.

[13] I. Salesnick, "Balanced GHM-like multiscaling functions," IEEE Signal Processing Letters, Vol. 6, No. 5, pp. 111-112, May 1999.

[14] Z. Wang and A. C. Bovik, "A Universal image quality index," IEEE Signal Proc. Letters, Vol. 9, No. 3, pp. 8184, March 2002.


[2] The authors would like to thank Prof. Rick Blum, ECE Department, Lehigh University, for kindly providing these two image pairs.

[3] The original image is produced using a simple cut-and-paste technique, taking physically the "*in focus*" areas of each source image.